Nucleation Particles in Diesel Exhaust: Composition Inferred from In Situ Mass Spectrometric Analysis

ARTICLE *in* ENVIRONMENTAL SCIENCE AND TECHNOLOGY · SEPTEMBER 2005

Impact Factor: 5.33 · DOI: 10.1021/es049427m · Source: PubMed

7 AUTHORS, INCLUDING:

Johannes Schneider
Max Planck Institute for Chemistry
180 PUBLICATIONS **4,496** CITATIONS
SEE PROFILE

Ulf Kirchner
Ford Motor Company
16 PUBLICATIONS **671** CITATIONS
SEE PROFILE

Volker Scheer
Ford Motor Company
41 PUBLICATIONS **1,431** CITATIONS
SEE PROFILE

Environ. Sci. Technol. **2005**, *39,* 6153−6161

Nucleation Particles in Diesel Exhaust: Composition Inferred from In Situ Mass Spectrometric Analysis

J. SCHNEIDER,* N. HOCK, S. WEIMER,† AND S. BORRMANN

Cloud Physics and Chemistry Department, Max Planck Institute for Chemistry, Institute for Atmospheric Physics, Johannes Gutenberg University, Mainz, Germany

U. KIRCHNER, R. VOGT, AND V. SCHEER

Ford Forschungszentrum Aachen GmbH, Germany

Mass spectrometric measurements of size and composition of diesel exhaust particles have been performed under various conditions: chassis dynamometer tests, field measurements near a German motorway, and individual car chasing. Nucleation particles consisting of volatile sulfate and organic material could be detected both at the chassis dynamometer test facility and during individual car chasing. We found evidence that if nucleation occurs, sulfuric acid/water is the nucleating agent. Low-volatile organics species condense only on the preexisting sulfuric acid/water clusters. Nucleation was found to depend strongly on various parameters such as exhaust dilution conditions, fuel sulfur content, and engine load. The latter determines the fraction of the fuel sulfur that is converted to sulfuric acid. The organic compounds (volatile and low-volatile) condense only on preexisting particles, such as both sulfuric acid nucleation particles and larger accumulation mode soot particles. On the latter, sulfuric acid also condenses, if the conditions for nucleation are not given. The overall ratio of sulfate to organic (volatile and low-volatile) is also strongly dependent on the engine load. It was found that the production of nucleation particles even at high engine load can be suppressed by using low-sulfur fuel.

1. Introduction

Understanding the processes of particle formation in diesel exhaust is of importance because of the discussion on adverse effects that diesel particles may have on human health. Diesel exhaust typically contains fine (D_p < 2.5 μm) and ultrafine (D_p < 0.1 μm) soot particles and, under certain conditions, nucleation particles (D_p < 0.05 μm) (*1*). Ultrafine particles reach deep into the lung and are therefore of special interest, although epidemiological studies with a focus on ultrafine particles are very sparse (*2*). The potential health effects of ultrafine solid and ultrafine soluble particles may be different, an aspect that has been neglected in epidemiological studies (*3*). Furthermore, particles from combustion processes may also influence the radiation budget of the atmosphere. It is presently under discussion whether particulate black carbon emissions contribute to the radiative forcing of the atmosphere on local scales or possibly also on a global scale (*4*) or whether the total short- and long-wave relaxed forcing by these aerosols remains near zero, as calculated by Penner et al. (*5*). The primary emissions of diesel engines include aerosol precursor gases (SO_2, SO_3, H_2SO_4, H_2O, low-volatile organic species, and semivolatile organic species) as well as soot particles, which are fractallike agglomerates of approximately solid spheres with diameters of about 20 nm (*1*, *6*). During the dilution and cooling process, a competition between nucleation of the low-volatile species and condensation on the surface of the existing particles occurs. A schematic of these processes is displayed in Figure 1. The fractallike soot particles have been observed to undergo compaction (*7*) when low- and semivolatile species condensate on their surface. This will result in higher density but lower diameter (mobility equivalent or aerodynamic) of the particles and less irregular shape. This accumulation mode (with soot particles as cores and various species as condensates) can be observed regularly during chassis dynamometer tests. The diameter of these particles ranges from about 50 to 500 nm (*1*, *8*, *9*). Under certain dilution conditions, nucleation particles with diameters in the range of 10−50 nm can be observed. This nucleation mode can be due to either nucleation of sulfuric acid water clusters or possibly also nucleation of low-volatile organics vapors, which might originate from lubricating oil. The latter pathway is indicated with the dotted line in Figure 1.

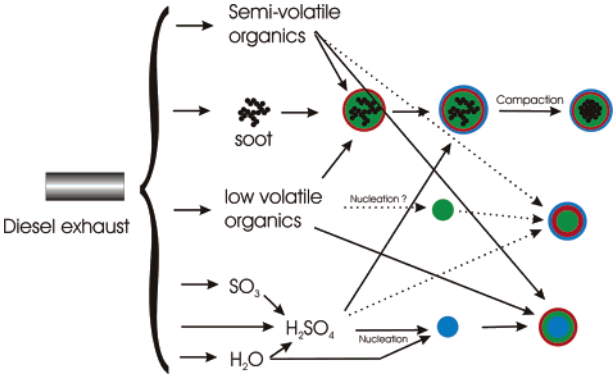

FIGURE 1. Schematic of the emissions and particle formation mechanisms in diesel exhaust. Solid lines indicate well-established processes, dotted lines indicate processes under discussion.

It is thought that the sulfuric acid/sulfate fraction in total mass emission is dependent on the fuel sulfur content, while the soluble organics fraction (SOF), consisting mainly of unburned fuel and lube oil, is strongly dependent on engine operating conditions and is highest from heavy-duty engines at light loads when exhaust temperatures are low (*1*). For light-duty diesel cars, Maricq et al. (*10*) and Vogt et al. (*11*) could show that both high sulfur and the oxidation catalyst are mandatory conditions for sulfate formation, which resulted in nucleation particle formation. Shi and Harrison (*12*) found that binary nucleation of sulfuric acid/water with subsequent condensation of organic substances explained qualitatively their observations in diesel exhaust, but the calculated nucleation rate was too low. To explain this discrepancy, they suggested that other species (e.g., ammonia) might be involved in the nucleation, while Yu (*13*) suggested that chemiions could play a role in diesel exhaust nucleation. Kleemann et al. (*14*) found significant amounts of ammonium in diesel exhaust particles and observed

* Corresponding author phone: +49 6131 305-586/596; fax: +49 6131 305-597; e-mail: schneider@mpch-mainz.mpg.de.

† Present addresses: EMPA, CH-8600 Dübendorf, Switzerland, and Paul Scherrer Institute, CH-5232 Villigen, Switzerland.

10.1021/es049427m CCC: $30.25
Published on Web 07/12/2005

nucleation particles ($D \approx 30-50$ nm) also when a low-sulfur fuel, containing 33 ppm sulfur by mass, was used.

Tobias et al. (*15*), who used a thermal desorption beam particle mass spectrometer (TDBPMS), investigated the composition of diesel exhaust particles and found evidence for sulfuric acid in nanoparticles. They concluded indirectly that because of the Kelvin effect it is unlikely that organic compounds alone are nucleating. Further mass spectrometric experiments on diesel exhaust particles have been reported by Suess and Prather (*16*) and Vogt et al. (*17*), but these were restricted to particles with diameters larger than 200 nm because of the light-scattering particle detection and can therefore give no insight into the nucleation process. By randomly chasing in-use buses in New York City and measuring their exhaust with an Aerodyne aerosol mass spectrometer (AMS), Canagaratna et al. (*18*) found sulfate and organics in the accumulation mode around 100 nm and a larger exhaust-related particle mode at around 500 nm, but they could not detect nucleation particles. Recently, Zhu et al. (*19*) and Kittelson et al. (*20*) investigated number density and size distribution of ultrafine particles near and on highways, but these studies did not include chemical analysis of the particles.

Here we report on various in situ measurements using the Aerodyne AMS with a modified inlet, allowing the analysis of particles with diameters as small as 20 nm. The measurements included chassis dynamometer tests, field measurements near a German Autobahn (motorway), and individual car chasing. Our experiments imply that sulfuric acid is the nucleating agent in diesel exhaust. Nucleation is strongly dependent on the dilution and the fuel sulfur content, but the amount of sulfate in the aerosol phase does also strongly depend on the engine load and exhaust gas after treatment (e.g. oxidation catalyst). The motorway traffic, however, did not produce significant amounts of aerosol sulfate. Nucleation particles, although present in the number size distribution between 10 and 20 nm, could not be detected and analyzed with the mass spectrometer. However, a significant amount of nonrefractory (volatile, semivolatile, and low-volatile) organic substances was found on accumulation mode soot particles.

2. Experimental Section

2.1. Instrumentation. The size-resolved chemical analysis has been carried out with the Aerodyne aerosol mass spectrometer (AMS). For a detailed description of the instrument, see refs *21*−*24*.

This instrument allows the quantitative measurement of volatile and semivolatile aerosol compounds, as sulfate, nitrate, ammonium, and organics (no black carbon), as well as chemically resolved size distributions, in a size range between 20 and 1500 nm. [The transmission efficiency of the inlet system, pinhole plus lens, calculated by Zhang et al. (*25*), is shown in the Supporting Information.] 100% transmission is reached for particles with aerodynamic diameters between 50 and 500 nm.

Since the acceleration of the particles in the aerodynamic lens takes place in the free molecular regime, the measured diameter is the so-called vacuum aerodynamic diameter D_{va}, which is related to the volume equivalent diameter D_V by

$$D_{va} = D_V \frac{\rho_p}{\rho_0} \frac{1}{\chi} \quad (1)$$

where ρ_p is the density of the particle, ρ_0 is the unit density, and χ is the dynamic shape factor (*26*, *27*).

The quantitative analysis of the mass loadings is described in detail by Allan et al. (*28*) and Alfarra et al. (*29*). Here, we focus on the sulfate and organic components of the exhaust

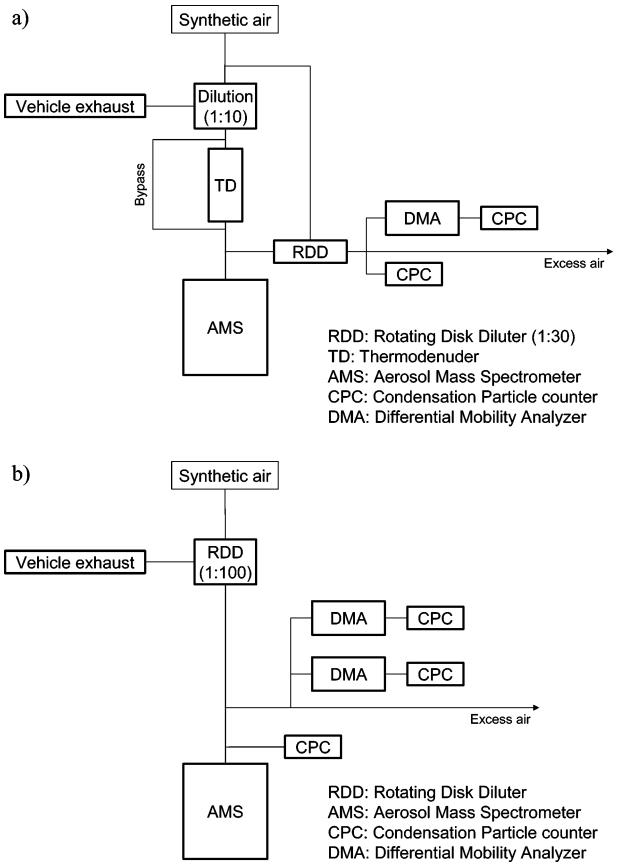

FIGURE 2. Setups during the dynamometer experiments. (a) Nucleation particle experiment; (b) engine load variation experiment. All connections were made of stainless steel tubes with an outer diameter of 6.35 mm (1/4 in.).

particles. Sulfate mass loadings are inferred from the ions SO^+, SO_2^+, SO_3^+, HSO_3^+, and $H_2SO_4^+$ ($m/z = 48$, 64, 80, 81, and 98). Organics are inferred from various mass peaks that are known not to originate from inorganic species such as sulfate, nitrate, ammonium, chloride, etc. Typical ion signals from organics molecules appear at the ion series $C_nH_{2n-1}^+$ and $C_nH_{2n+1}^+$. Also, multiple contributions to individual mass peaks, inferred from laboratory data, are accounted for (*28*).

Additional instrumentation included two scanning mobility particle sizers (TSI 3080 and 3934) and condensation particle counters (TSI 3025 and 3022).

2.2. Sampling Locations: *2.2.1. Test at the Chassis Dynamometer Facility at Ford Research Center Aachen.* The tests were performed on a 48 in. (1.22 m) diameter concrete roll ("Compact Rolle", AVL, Kiel, Germany) with maximum 186 kW brake power, maximum speed 200 km h^{-1}, and loss compensation. For the experiments, two different diesel passenger cars were used: a model year 2000, 1.8 L, 66 kW (90 hp) car and a model year 2002, 1.8 L, 74 kW (100 hp) car with common rail direct injection technique. Both cars were equipped with a turbo charger, exhaust gas recirculation, and oxidation catalyst. The vehicle inertia weights were both 1360 kg, and emission levels were Euro-III. The sampling configuration of the instruments is shown in Figure 2. The length of the sampling line (stainless steel) between the exhaust pipe and the AMS was about 2 m, corresponding to a residence time of the particles in the flow tube of less than 1 s.

2.2.2. In Situ Measurements at Motorway A4 near Aachen. These measurements were conducted at a parking lot adjacent to the motorway (Autobahn) A4 (four-lane high-speed highway with significant heavy-duty diesel traffic) on

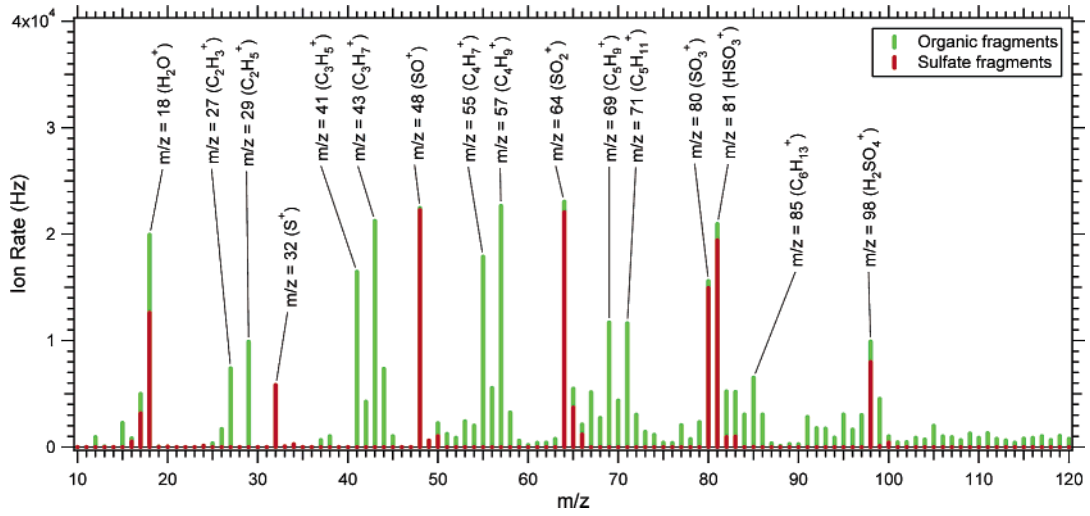

FIGURE 3. Mass spectrum of aerosol particles, recorded on the chassis dynamometer (section 3.2.2) with 360 ppm sulfur fuel, at 120 km/h and an engine load of 15 kW. Contributions of gas-phase ions (mainly N^+, N_2^+, O^+, O_2^+, and Ar^+) have been removed for clarity. Major peak components are identified; coloring refers to the origin of the ionic fragments [inferred from laboratory data by Hogrefe et al. (*30*)].

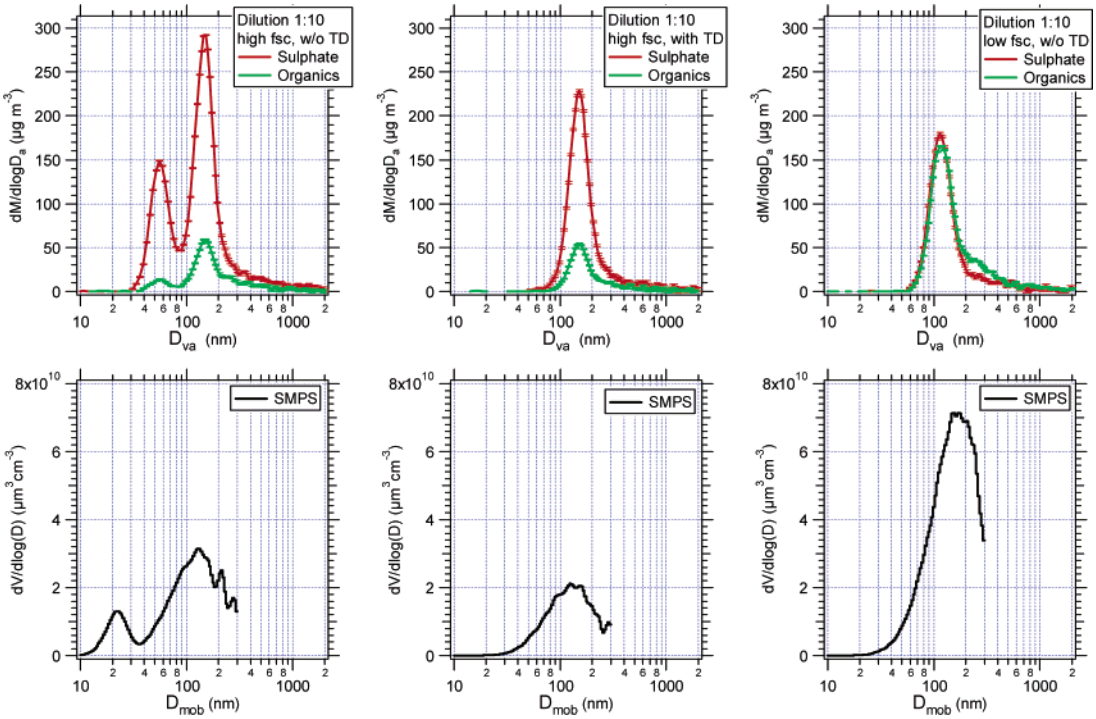

FIGURE 4. Nucleation particles in diesel exhaust: upper row, AMS data; lower row, SMPS data. Left panels: Bimodal size distribution, containing sulfate and organics, produced with a dilution ratio of 1:10 and a high fuel sulfur content of 360 ppm. Middle panels: same experiment, but with thermodenuder between diluter and AMS. Right panels: Experiment with low fuel sulfur content (2 ppm), without thermodenuder.

Monday, Tuesday, and Wednesday, February 17, 18, and 19, 2003, between 10:00 and 18:00. For this purpose the AMS was integrated into the Ford Mobile Laboratory (FML) (*17*), which is a mobile experimental platform based on a Ford transit van. It is equipped with a scanning mobility particle sizer (SMPS, model 3934L, TSI Inc.), a condensation particle counter (CPC model 3022, TSI Inc.), CO and NO_x analyzers (models 300 and 200A, API), and data acquisition instruments. Sampling was performed through a 4 mm i.d. stainless steel inlet in front of the radiator grill. A 10.3 mm i.d. stainless steel line of 420 cm length connected the sampling probe with the inside of the FML. Air was drawn at a volume flow of 17 L min^{-1}, from which the filtered sheath air for the SMPS was taken and the instruments sampled at their specified flow rates. The residence time inside the stainless steel line was 1.2 s. The different response and delay times of the gas and aerosol analyzers were adjusted further downstream.

The FML was situated 16 m to the south of the motorway, which runs in an east−west direction. Throughout the three measurement days, the wind direction remained stable between 60° and 90° (east northeast). Since the wind speed was very low on these days (average 1.2 m/s on Feb 18 and 0.9 m/s on Feb 19), and the wind direction varied inside the above-mentioned range, the residence time of the emissions before reaching the sampling tubes was between 60 and 500 s.

Electrical power was supplied by a diesel power generator, which was placed 50 m away downwind. On a weekday, the

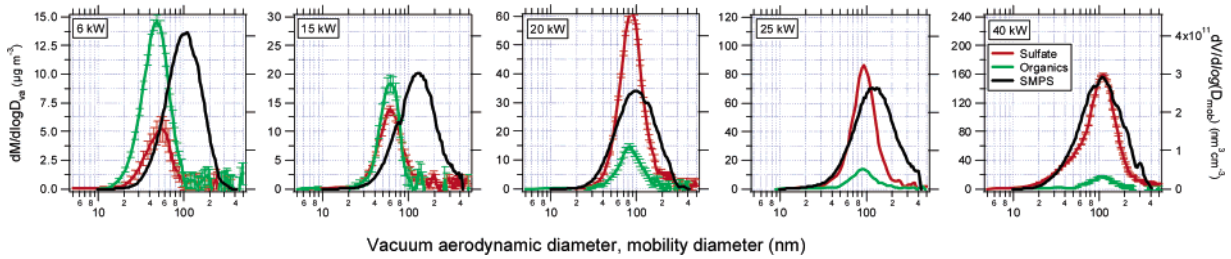

FIGURE 5. Mass distribution of organics and sulfate (left scale) obtained on the chassis dynamometer test site at different engine loads at a speed of 120 km/h (FSC = 360 ppm). Also shown is the volume distribution measured with the SMPS system (right scale).

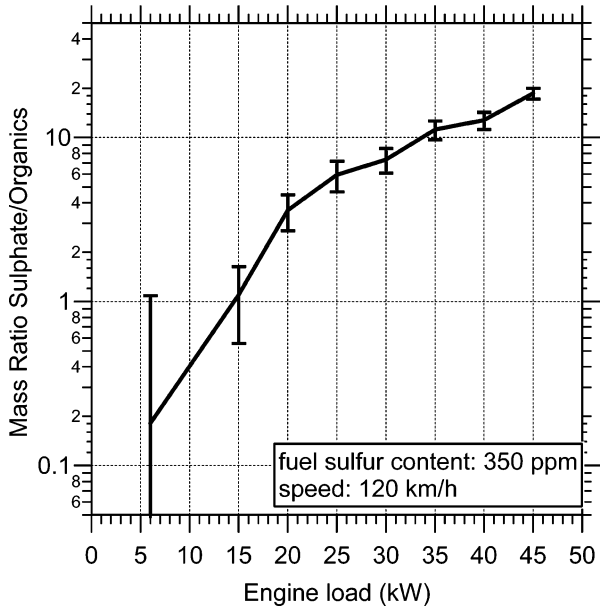

FIGURE 6. Mass ratio of sulfate to organics contained in the diesel exhaust particles as a function of the engine load as measured with the AMS.

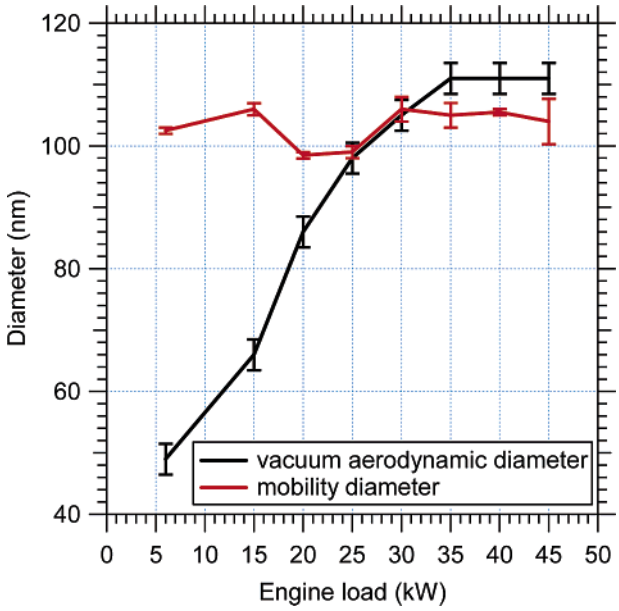

FIGURE 7. Vacuum aerodynamic diameter and mobility diameter of the exhaust particles as a function of the engine load.

typical traffic volume on both lanes is approximately 2500 (+1500/−500) passenger cars per hour and approximately 750 (± 250) heavy-duty diesel trucks per hour (*17*). The slope of the lane close to the parking lot is ca. 1% uphill, speed limit is 120 km/h.

To identify the contribution of the traffic-related aerosol to the total aerosol, on Thursday, February 20, between 10:00 and 18:00, a background measurement was performed at a rural site, about 3 km north from the highway and 0.6 km from the small village Dürwiss, near the lake Blausteinsee.

2.2.3. Vehicle Test Track. For individual car-chasing experiments a vehicle was followed by the Ford Mobile Laboratory (FML) on the Ford test track at a constant distance as described in detail in Vogt et al. (*11*). Briefly, the test track was an oval of 4 km length per lap. To avoid interference from other sources, no other vehicles were allowed on the test track during all measurements. In the FML a battery pack and an on-board supply were installed, which allowed operation of the instruments while driving.

3. Results

3.1. General. Figure 3 gives a mass spectrum recorded with the AMS in mass spectrometric (MS) mode at the chassis dynamometer during the engine load variation experiment (see section 3.2.2), at an engine load of 15 kW, using diesel fuel with 360 ppm sulfur mass content. The ions are classified and colored according to their parent molecules into organics and sulfate. Multiple assignments of certain peaks rely on fragmentation patterns inferred from laboratory work (*24*, *30*). The spectra are similar to those reported by Canagaratna et al. (*18*) using an Aerodyne AMS and Tobias et al. (*15*) using a TDPBMS. The height of the sulfate peaks showed a significant dependence on the engine load, a finding that will be discussed in more detail in section 3.2.2.

The major peaks identified in Figure 3 were used to determine the size distribution of organics (m/z 41, 43, 55, and 57) and sulfate (m/z 48 and 64) in the time of flight (ToF) mode. For the following analyses, only ToF-mode data will be used. A more detailed comparison between mass spectra recorded from diesel fuel, unburned diesel fuel, lube oil, and other combustion particles will be presented in a separate paper (*31*).

3.2. Chassis Dynamometer Results: *3.2.1. Nucleation Particles.* For this experiment, the 74 kW common rail diesel passenger car was operated at a speed of 120 km/h and a load of 20 kW, corresponding to a flat road without slope. Two fuels with different fuel sulfur content were used (360 and 2 ppm). To change from high to low fuel sulfur, the tank was drained and the engine was run about 10 min with the low-sulfur fuel until it was fully cleared of the remainders of the high-sulfur fuel.

When the exhaust gas was diluted by a factor of 10 directly behind the exhaust pipe (see Figure 2a) and the engine was operated with the high-sulfur fuel, a large number of nucleation particles were produced. The left panel of Figure 4 shows the mass distribution $dM/d(\log D_p)$ of organics and sulfate measured with the AMS in TOF mode, averaged over 600 s. Both organics and sulfate size distributions are bimodal. We term the small mode (with $D_{va} \approx 55$ nm) "nucleation mode" and the second mode "soot particle mode". The ratio between sulfate and organics in the nucleation mode is about

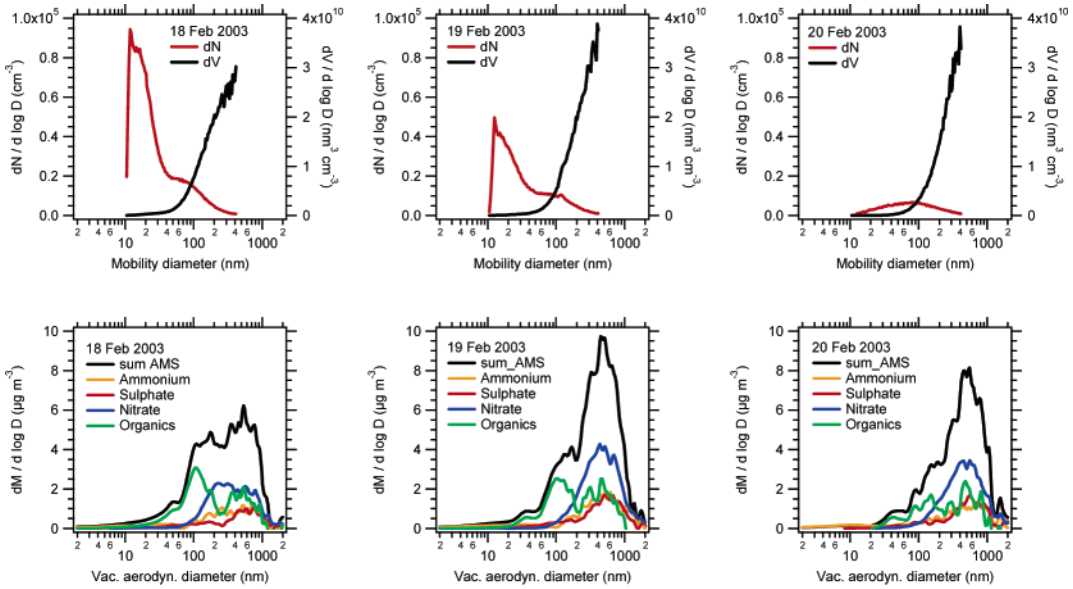

FIGURE 8. Number and volume distribution measured with the SMPS (upper panel) and mass distributions measured with the AMS (lower panel) during February 18 and 19 (12:00−18:00) on the parking lot close to the motorway and on February 20 at a remote location, 5 km away in northerly direction.

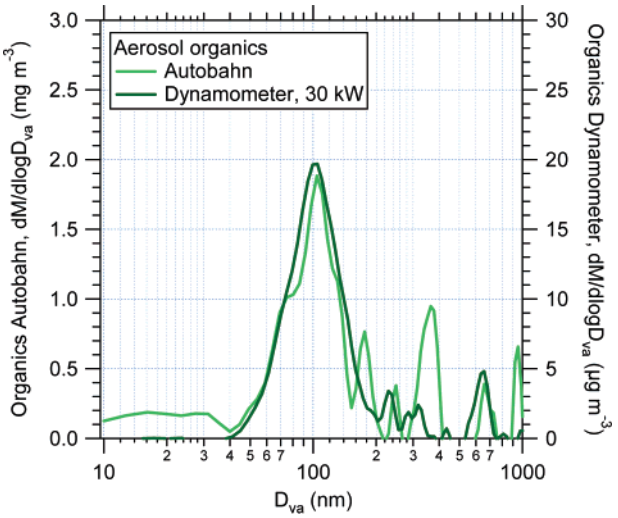

FIGURE 9. Traffic contribution of organics measured at the Autobahn (natural background subtracted) compared to a diesel passenger car run on the chassis dynamometer test run at 120 km/h and 30 kW engine load.

11, while it is about 5 for the soot particle mode. The lower row of Figure 4 shows the corresponding SMPS data.

To verify that this particle mode is indeed formed by nucleation and not by condensation on preexisting primary soot spheres, a thermodenuder operating at 280 °C [as described in Wehner et al. (*32*)] was inserted in the sampling line. (When sampling was done without the thermodenuder, a bypass of the same length was used to eliminate the risk of ambiguities due to possible sampling line losses.)

The middle panel of Figure 4 shows the size distributions of sulfate and organics with a dilution ratio of 1:10 measured with the thermodenuder inserted. The small mode disappears completely, from which we conclude that it is indeed a nucleation mode and does not contain refractory material such as soot.

A second experiment was conducted under the same conditions but with low-sulfur fuel (2 ppm). The results are given in the right panel of Figure 4. Again, no nucleation mode is observed. Furthermore, the amount of organics condensed on the soot particle mode has increased. This finding indicates that the formation of the nucleation mode is triggered by sulfuric acid. If the low-volatile organic compounds were the nucleating agent, the nucleation mode should also be present in the low-sulfur experiment. However, the low- and semivolatile organic substances seem to condense in this case only on the accumulation mode soot particles when no small sulfuric acid nuclei are available.

A comparison of AMS and SMPS size distributions (lower panel in Figure 4) shows that the soot particle mode is measured at nearly the same vacuum aerodynamic and mobility diameter but the AMS size distribution is much sharper. Laboratory measurements of graphite soot particles have shown that the vacuum aerodynamic diameter becomes almost independent of the mobility diameter if the particles are fractal-shaped (*31*, *33*). This might explain the difference in the width of the size distributions of the soot particle mode. The mode diameters of the nucleation modes reveal a ratio of $D_{va}/D_{mob} = 55.3\ nm/22.1\ nm = 2.5$. Since we assume the nucleation particles to be spherical, this implies a density of 2.5 g cm^{-3} (see eq 1). This is larger than the expected density of pure H_2SO_4 (1.83 g cm^{-3}), diesel, and lubrication oil. Typical density values for lubrication oil are in the range between 0.9 and 1.0 g cm^{-3}, and for diesel, between 0.85 and 0.88 g cm^{-3}. At present there is no explanation for this difference. Furthermore, the absolute volume and mass concentrations measured with both AMS and SMPS agree that in the low fuel sulfur case the volume and the nonrefractory organic mass of the emitted particles are higher than they are in the high fuel sulfur case.

Tobias et al. (*15*) concluded from their measurements that sulfuric acid is the nucleating agent, followed by condensation of low- and semivolatile organic compounds. This agrees with our findings. However, we find a much larger content of sulfate/sulfuric acid in the nucleation particles than did Tobias et al. While they inferred a mass fraction of up to 5%, we measure a mass fraction of about 90% sulfate and only 10% organics. These mass ratios, however, are thought to depend strongly on the presence of an oxidation catalyst, the engine type, the fuel sulfur content, and the dilution ratio, which determines the amount of organic material that is able to condense on the nucleation particles. Since Tobias et al. used a completely different engine type (4.5 L displacement, used for short-duration heavy lifting, in contrast to our 1.8 L displacement passenger car), a direct

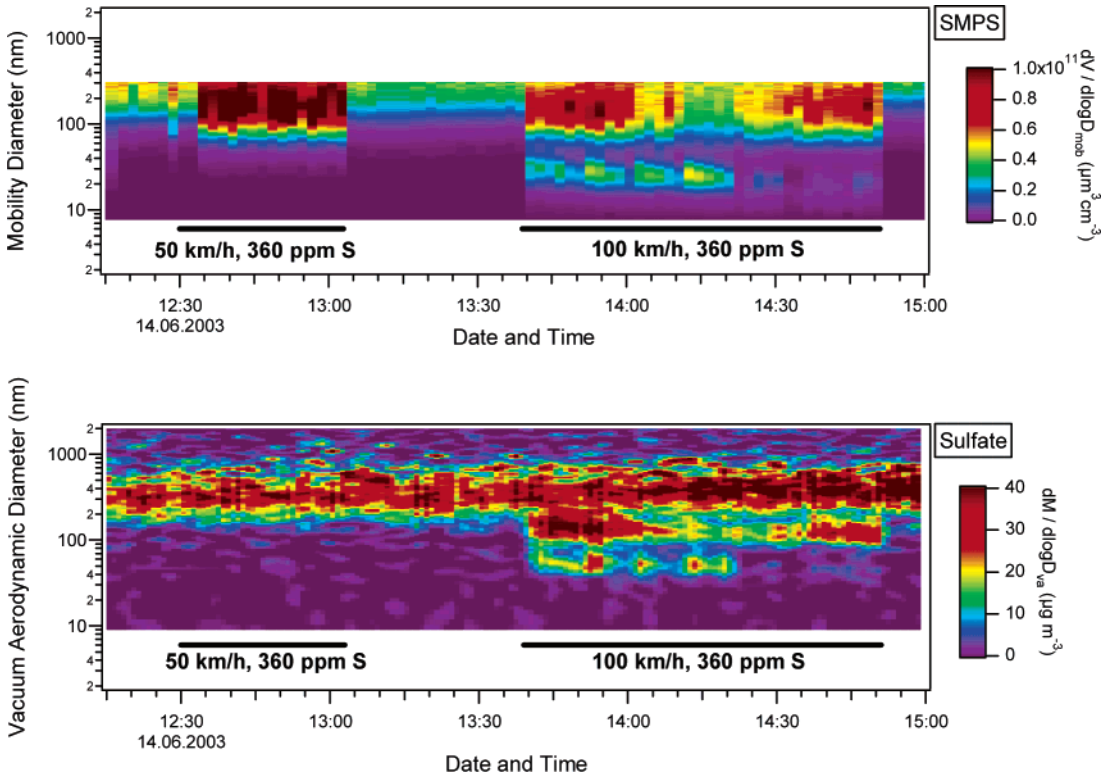

FIGURE 10. Volume size distribution measured with the SMPS (top panel) and mass size distribution of sulfate measured with the AMS during the individual car chasing. Displayed are two chasing events (indicated by bars), at 50 km/h and 100 km/h, each measured at a distance of 10 m. The fuel sulfur content was 360 ppm.

comparison of our results and those reported by Tobias et al. is not possible and would lead to erroneous conclusions.

Shi and Harrison (*12*) found that binary H_2SO_4−H_2O nucleation could not explain the high observed nucleation rate and proposed a third substance that could be ammonia or some organic compound playing a role. The AMS is able to detect ammonium at the mass peaks $m/z = 15$ and 16 (NH^+ and NH_2^+), two peaks that also have significant contributions from organics and gas-phase oxygen. Even though we could not detect ammonium in the particle phase, a statement about the composition of the fresh nucleation core cannot be made, since the AMS is sensitive only to particles with $D_{va} > 20$ nm and the amount of ammonia may be too low to be detected by the AMS if the particles have grown due to condensation of sulfuric acids and low-volatile organic compounds. Thus, it cannot be ruled out that, in the early state of particle formation, ammonia is involved.

3.2.2. Dependence of the Sulfate Conversion on the Engine Load. This experiment was performed with the 66 kW diesel car. At a dilution ratio of 1:100 (realized by a different setup, as given in Figure 2b), no nucleation particles were observed. We chose this setting to study the influence of the engine load on the particle composition and size. Figure 5 shows mass distributions of the organic and sulfate content of the aerosol particles obtained with the AMS at different engine loads (6−45 kW). Also given are the volume distributions measured with the SMPS systems. This test was performed with a fuel sulfur content (FSC) of 360 ppm.

While the mass concentration of organic substances remains almost constant with increasing engine load, the sulfate mass concentration markedly increases. The ratio of sulfate to organics versus engine load is displayed in Figure 6. The increase of aerosol sulfate with increasing engine load can be explained as follows:

Most of the fuel sulfur is oxidized to SO_2 during the combustion process. However, on the surface of the oxidation catalyst, which is designed to oxidize CO and organics substances to CO_2, SO_2 is further oxidized to SO_3, which rapidly reacts with H_2O to form H_2SO_4. The extent of this undesired reaction depends on the catalyst formulation. In our experiment the conversion efficiency of SO_2 to SO_3 depends on the temperature of the oxidation catalyst, which in turn depends on the engine load, since the exhaust gas temperature increases with increasing engine load.

Furthermore, Figure 5 reveals that the vacuum aerodynamic diameter D_{va} (the diameter measured with the AMS; see eq 1) increases with engine load, while the mobility diameter D_{mob} (measured with the SMPS) remains constant. The modal diameters measured with both instruments are plotted as a function of engine load in Figure 7. The density and shape of the particles depend on the composition: First, a higher content of sulfuric acid increases the density ($\rho_{H_2SO_4} > \rho_{diesel}, \rho_{lubeoil}$); second, the condensation of organic vapors and/or sulfuric acid on soot particles leads to "compaction" (*7*) or at least to a spherical outer shell of the soot particles (see Figure 1). A nonspherical particle means a shape factor larger than 1 and thereby a smaller D_{va}. A higher density, in turn, leads to a higher D_{va}. Thus, both processes (shape becomes spherical, density increases) lead to an increase of D_{va}.

3.3. Results from Field Studies: *3.3.1. Measurements near a Motorway.* The upper panel of Figure 8 shows the number and volume distributions measured with the SMPS during the motorway experiment. On February 18 and 19, when measurements were taken at the parking lot located directly at the motorway, the number distribution shows a distinct peak between 10 and 40 nm that does not show up in the volume distribution. This peak is not present on February 20, when background air (5 km northeast of the parking lot) was sampled.

The mass distributions measured by the AMS do not reveal the nucleation peak, since the mass concentrations of these particles are too small, and particles below 20 nm are not detected.

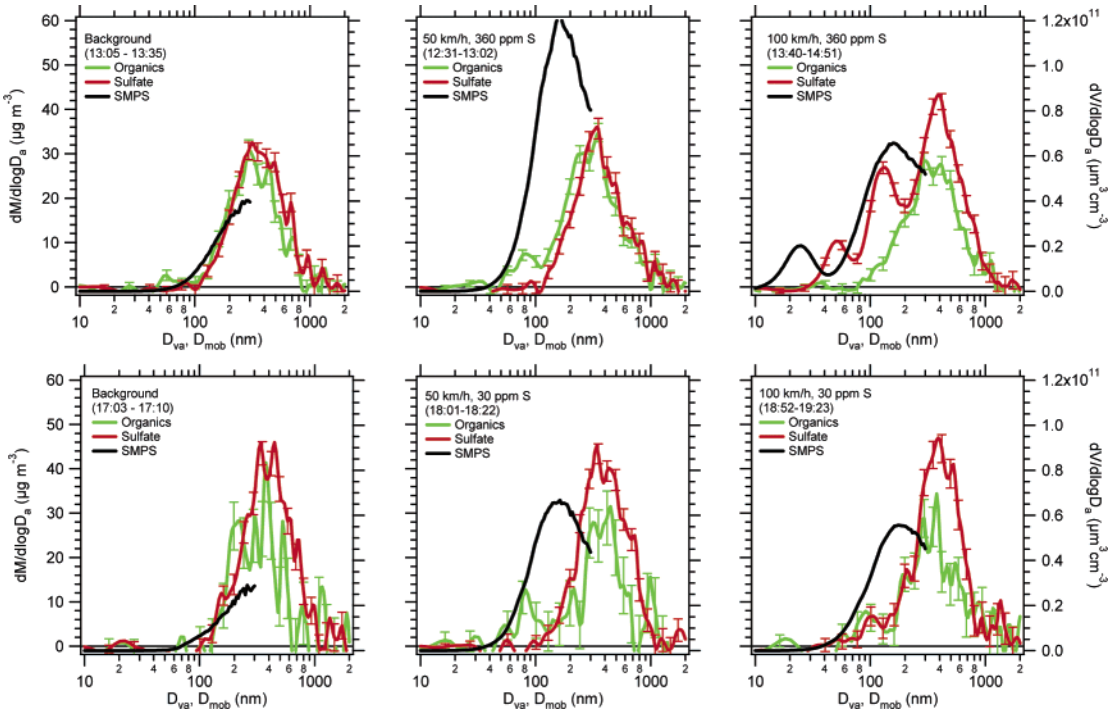

FIGURE 11. Mass size distributions of sulfate and organics (left scale) measured with the AMS and volume size distributions measured with the SMPS (right scale) during individual chasing of a diesel car at a distance of 10 m at two speeds, 50 and 100 km/h. Upper panel, high FSC (360 ppm); lower panel, low FSC (30 ppm). The background curves (left) were recorded directly before and between the car chasings.

However, a traffic-associated contribution can be found in the organic species measured by the AMS: While the size distributions of sulfate, nitrate, and ammonium are very similar on the three days, the organic particle mode at 100 nm is much more pronounced close to the motorway than in the background. It is important to emphasize that this is the accumulation mode, since the nucleation particles did not contain enough mass to be detected by the AMS.

The SMPS volume distribution corresponds roughly to the sum of all species measured with the AMS, but it must be taken into account that only the nonrefractory part of the aerosol can be detected by the AMS. Also, the different densities and possibly also shapes of externally mixed organic and inorganic particles such as ammonium nitrate and ammonium sulfate may cause a different shape of the SMPS volume distribution and the AMS mass distribution, since the SMPS refers to mobility equivalent diameter and the AMS to vacuum aerodynamic diameter.

To compare this field result to the chassis dynamometer findings, the background size distribution of the organics, measured on February 20, was subtracted from the average size distributions obtained on the two motorway days. In Figure 9 this "traffic-only" organic aerosol mode is compared to the chassis dynamometer results from the 30 kW run that was measured during the experiment described in section 3.2.2. This engine load setting matches best the distribution width and the mode diameter measured next to the motorway. The broad mode below 40 nm is not regarded to represent nucleation particles, since their distribution looks completely different than that discussed in section 3.2.1.

For the measured sulfate size distribution, the same differential "traffic-only" size distribution was calculated. However, no significant sulfate mass concentration contributed from the motorway traffic was found. In contrast, during the dynamometer measurements generally more sulfate mass than organic mass was found in the exhaust of a single passenger car (see Figure 6), if the engine load exceeded 15 kW. However, the fuel sulfur content (FSC) during this experiment was 360 ppm, which is about 7 times more than is contained in today's commonly used fuel. The FSC was reduced by European legislation to 350 ppm since 2000, and to 50 ppm from 2005 on, while in Germany, 50 ppm fuel has been sold since 2001 and 10 ppm fuel since 2003. Eastward-going trucks in transnational traffic, however, have been fueled up most likely in other European countries since the measurement location was close to Germany's western border.

Furthermore, the motorway exhaust is dominated by heavy-duty traffic. It might be that these engines, which are often not equipped with an oxidation catalyst, emit more organic matter (unburned fuel or lubrication oil) than sulfate. Finally, it is likely that the traffic mix of heavy-duty trucks and old and new passenger cars emits on average more unburned low- and semivolatile organic substances than a modern, Euro-III engine as it was used on the chassis dynamometer.

3.3.2. Individual Car Chasing. A single test car was followed under ambient conditions with the mobile lab (FML). These experiments were carried out in June 2003 on a test track. Like during the motorway experiment, the mass spectrometer, together with the SMPS, was located in the FML. MS- and ToF-mode data were taken with 60 s time resolution, while the SMPS was scanning within 120 s between 7 and 300 nm. During the experiment, the 74 kW diesel car (the same car as in section 3.2.1) was closely followed at various speeds at a distance of 10 m. Here, fuels 360 and 30 ppm were used successively. Background measurements (i.e., driving on the test road and collecting data without a test car) were performed before (and/or after) each chasing experiment. The dilution factor for this experiment was calculated from CO_2 measurements to be around 900.

The upper panel of Figure 10 gives the SMPS volume distribution; the lower panel gives the mass distribution of sulfate as a function of time during two chasing experiments when the car was running on the 360 ppm fuel. The periods when the Ford Mobile Lab was driving 10 m behind the test

vehicle are indicated by the bars. Between these chasing events, the Mobile Lab was continuing on the test road while the test vehicle was parking. After reentering the test road, the test vehicle stayed behind the Mobile Lab until both reached 100 km/h. Then the test vehicle overtook the Mobile Lab and the next chasing phase started.

The background aerosol between $D_{va} = 200$ and 800 nm is present throughout the whole time span, and its size and mass concentration are increasing slightly during the displayed time frame. The SMPS can only detect the smaller fraction of these particles since it was scanned only up to 300 nm. The indicated chasing episode at 50 km/h induces a marked increase of the SMPS number concentration above 70 nm, while it does not induce a noticeable change in the sulfate aerosol. Coincidentally with the start of the 100 km/h chasing phase, two additional sulfate modes appear at about 50 and 130 nm, respectively. After the end of the chasing phase, the two modes disappear immediately. These small sulfate particle modes occurred most pronounced only in the 100 km/h, 360 ppm S case, as shown in Figure 11. Here the averaged size distributions of sulfate and organics during the 50 km/h and 100 km/h chasing events are given together with background measurements immediately before or between the chasing events and the corresponding SMPS volume distributions. The 100 km/h chasing events are displayed on the right. When low-sulfur fuel was used (30 ppm, lower row), the exhaust particle mode around 100 nm is markedly smaller than in the high-sulfur case (upper row). Interestingly, an additional organic particle mode (around 100 nm) appears in the low-sulfur case when driving 100 km/h that is not observed with the high fuel sulfur content. This finding agrees with the experiment described in section 3.2.1. At 50 km/h, sulfate particles are not formed, with low or high sulfur, but again, the organic particles show a distinct accumulation mode (or soot particle mode) at around 80 nm. It seems that at lower speed the engine emits more unburned hydrocarbons than it does at higher speed.

The difference between the D_{mob} and D_{va} of the nucleation mode of about a factor of 2 agrees with the assumption that these particles are composed of sulfuric acid (density 1.83 g cm^{-3}). In the 50 km/h cases the SMPS observes much more particle volume in the accumulation mode, since the AMS cannot vaporize the soot particles but only the condensed species on their surfaces. The particle volume concentration of the accumulation mode measured with the SMPS decreases when the diesel car is driven at higher speed. The accumulation mode is observed at a higher mobility diameter compared to the vacuum aerodynamic diameter, a finding that suggests that these particles are mainly composed of soot, therefore having a lower density and a higher shape factor than the sulfuric acid-dominated particles found in the nucleation mode.

Figure 12 gives a comparison between the sulfate nucleation particles observed on the chassis dynamometer (120 km/h, 360 ppm S; see section 3.2.1) and the nucleation particles observed during the chasing (100 km/h, 360 ppm S). The data have been corrected for the different dilution ratios (chassis dynamometer 1:10; test road ≈ 1:900). The time scales between emission and measurement are similar for both experiments (dynamometer 1 s; chasing 1.5 s). It appears that both size distributions look very similar, only that the accumulation mode is slightly larger for the dynamometer data. The absolute concentrations, in contrast, are much larger in the chasing experiment than at the dynamometer. However, atmospheric dilution and chassis dynamometer dilution are not directly comparable since the chassis dynamometer dilution uses particle-free air while under normal atmospheric conditions (motorway, city traffic) the particle concentration in the ambient air is on the order of 10^4 cm^{-3}.

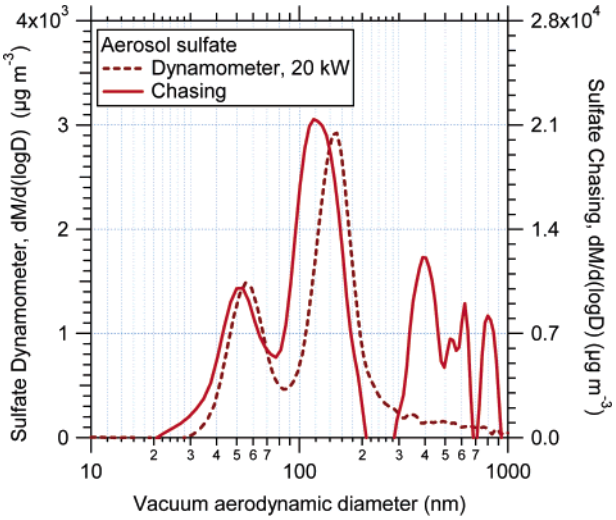

FIGURE 12. Comparison between the sulfate mass distributions measured at the chassis dynamometer (left scale) and during the single car chasing (right scale, background subtracted). The data have been corrected for dilution (dynamometer 10; chasing 900).

Summarizing, we found that the formation of nucleation mode particles from diesel exhaust occurs only under certain conditions: high fuel sulfur content, high engine load, and an appropriate exhaust gas dilution. The fuel sulfur content and the engine load determine the available sulfuric acid in the exhaust gas. The formation of nanoparticles could be successfully suppressed when low-sulfur fuel was used, indicating that the nucleation is triggered by sulfuric acid and not by low-volatile organics, which condense only later on the freshly nucleated cores.

Nucleation particles form by gas-to-particle conversion after the exhaust gas has left the exhaust pipe. Particle traps are known to effectively remove soot particles and are not designed to remove nucleation particles.

Since nucleation particles are completely volatile and do not have a solid soot core, their health effects might be different from those of particles with a solid core. Future health effect studies should clearly distinguish between chemically different particles in the ultrafine size range.

Acknowledgments

The authors thank Thomas Böttger for technical support during the measurements, James Allan and all contributors to the AMS analysis toolkit, the AMS community for many helpful discussions, and two anonymous reviewers for their comments.

Supporting Information Available

Figure showing transmission efficiency. This information is available free of charge via the Internet at http://pubs.acs.org.

Literature Cited

(1) Kittelson, D. B. Engines and Nanoparticles: A Review. *J. Aerosol Sci.* **1998**, *29*, 575−588.

(2) Oberdörster, G. Pulmonary effects of inhaled ultrafine particles. *Int. Arch. Occup. Environ. Health* **2001**, *74*, 1−8.

(3) Wichmann, H.-E.; Spix, C; Wölke, Th. Tuch, G.; Peters, A.; Heinrich, J.; Kreyling, W. G.; Heyder, J. Daily Mortality and Fine and Ultrafine Particles in Erfurt, Germany Part I: Role of Particle Number and Particle Mass. Health Effects Institute: Cambridge, MA, 2000; Research Report 98.

(4) Jacobson, M. Z. Control of fossil-fuel particulate black carbon and organic matter, possibly the most effective method of slowing global warming. *J. Geophys. Res.* **2002**, *107* (D19), 4410; doi 10.1029/2001JD001376.

(5) Penner, J. E., S. Y. Zhang, and C. C. Chuang, Soot and smoke aerosol may not warm climate. *J. Geophys. Res.* **2003**, *108* (D21), 4657; doi 10.1029/2003JD003409.
(6) Maricq, M. M.; Podsiadlik, D. H.; Chase, R. E. Size Distributions of Motor Vehicle Exhaust PM: A Comparison Between ELPI and SMPS Measurements. *Aerosol Sci. Technol.* **2000**, *33*, 239−260.
(7) Saathoff, H.; Naumann, K.-H.; Schnaiter, M.; Schöck, W.; Möhler, O.; Schurath, U.; Weingartner, E.; Gysel, M.; Baltensperger, U. Coating of soot and $(NH_4)_2SO_4$ particles by ozonolysis products of α-pinene. *J. Aerosol Sci.* **2003**, *34*, 1297−1321.
(8) ACEA programme on emissions of fine particles from passenger cars. ACEA: Brussels, Belgium, 1999.
(9) ACEA programme on emissions of fine particles from passenger cars [2]. ACEA: Brussels, Belgium, 2002.
(10) Maricq, M. M.; Chase, R. E.; Xu, N.; Laing, P. *Environ. Sci. Technol.* *36* **2002**, 283−289.
(11) Vogt, R.; Scheer, V.; Casati, R.; Benter, Th. On-road measurement of particle emission in the exhaust plume of a Diesel passenger car. *Environ. Sci. Technol.* **2003**, *37*, 4070−4076.
(12) Shi, J. P.; Harrison, R. M. Investigation of Ultrafine Particle Formation during Diesel Exhaust Dilution. *Environ. Sci. Technol.* **1999**, *33*, 3730−3736.
(13) Yu, F. Chemiion evolution in motor vehicle exhaust: Further evidence of its role in nanoparticle formation. *Geophys. Res. Lett.* **2002**, *29*, 15; doi 10.1029/2002GL015004.
(14) Kleemann, M. J.; Schauer, J. J.; Cass, G. R. Size and Composition Distribution of Fine Particulate Matter Emitted from Motor Vehicles. *Environ. Sci. Technol.* **2000**, *34*, 1132−1142.
(15) Tobias, H. J.; Beving, D. E.; Ziemann, P. J.; Sakurai, H.; Zuk, M.; McMurry, P. H.; Zarling, D.; Watylonis, R.; Kittelson, D. B. Chemical Analysis of Diesel Engine Nanoparticles Using a Nano-DMA/Thermal Desorption Particle Beam Mass Spectrometer. *Environ. Sci. Technol.* **2001**, *35*, 2233−2243.
(16) Suess, D. T.; Prather, K. A. Reproducibility of Single Particle Chemical Composition during a Heavy Duty Diesel Truck Dynamometer Study. *Aerosol Sci. Technol.* **2002**, *36*, 1139−1141.
(17) Vogt, R.; Kirchner, U.; Scheer, V.; Hinz, K. P.; Trimborn, A.; Spengler, B. Identification of diesel exhaust particles at an Autobahn, urban and rural location using single-particle mass spectrometry. *J. Aerosol Sci.* **2003**, *34*, 319−337.
(18) Canagaratna, M. R.; Jayne, J. T.; Ghertner, D. A.; Herndon, S.; Shi, Q.; Jimenez, J. L.; Silva, Ph. J.; Williams, P.; Lanni, Th.; Drewnick, F.; Demerjian, K. L.; Kolb, Ch. E.; Worsnop, D. R. Chase Studies of Particulate Emissions from in-use New York City Vehicles. *Aerosol Sci. Technol.* **2004**, *38*, 555−573.
(19) Zhu, Y.; Hinds, W. C.; Kim, S.; Shen, S.; Sioutas, C. Study of ultrafine particles near a major highway with heavy-duty diesel traffic. *Atm. Environ.* **2002**, *36*, 4323−4335.
(20) Kittelson, D. B.; Watts, W. F.; Johnson, J. P. Nanoparticle emissions on Minnesota highways. *Atm. Environ.* **2004**, *38*, 9−19.
(21) Jayne, J. T.; Leard, D. C.; Zhang, X.; Davidovits, P.; Smith, K. A.; Kolb, C. E.; Worsnop, D. R. Development of an aerosol mass spectrometer for size and composition analysis of submicron particles. *Aerosol Sci. Technol.* **2000**, *33*, 49−70.
(22) Jimenez, J. L.; Jayne, J. T.; Shi, Q.; Kolb, C. E.; Worsnop, D. R.; Yourshaw, I.; Seinfeld, J. H.; Flagan, R. C.; Zhang, X.; Smith, K. A.; Morris, J.; Davidovits, P. Ambient Aerosol Sampling with an Aerosol Mass Spectrometer. *J. Geophys. Res.* **2003**, *108*, 8425; doi 10.1029/2001JD001213.
(23) Allen, J. D.; Jimenez, J. L.; Coe, H.; Bower, K. N.; Williams, P. I.; Worsnop, D. R. Quantitative Sampling Using an Aerodyne Aerosol Mass Spectrometer. Part 1: Techniques of Data Interpretation and Error Analysis. *J. Geophys. Res.* **2003**, *108*, 4090; doi 10.1029/2002JD002358
(24) Schneider, J.; Borrmann, S.; Wollny, A. G.; Bläsner, M.; Mihalopoulos, N.; Oikonomou, K.; Sciare, J.; Teller, A.; Levin, Z.; Worsnop, D. R. Online mass spectrometric aerosol measurements during the MINOS campaign (Crete, August 2001). *Atmos. Chem. Phys.* **2004**, *4*, 65−80.
(25) Zhang, X.; Smith, K. A.; Worsnop, Jimenez, J. L.; Jayne, J. T.; D. R., Kolb, C. E.; Morris, J.; Davidovits, P. Characterization of Particle Beam Collimation: Part II. Integrated Aerodynamic Lens-Nozzle System. *Aerosol Sci. Technol.* **2004**, *38*, 619−638.
(26) Jimenez, J. L.; Bahreini, R.; Cocker, D. R., III; Zhuang, H.; Varutbangkul, V.; Flagan, R. C.; Seinfeld, J. H.; O'Dowd, C. D.; Hoffmann, T. New particle formation from photooxidation of diiodomethane (CH_2I_2). *J. Geophys. Res.* **2003**, *108* (D10), 4318; doi 10.1029/2002JD002452.
(27) Jimenez, J. L.; Bahreini, R.; Cocker, D. R., III; Zhuang, H.; Varutbangkul, V.; Flagan, R. C.; Seinfeld, J. H.; O'Dowd, C. D.; Hoffmann, T. Correction to "New particle formation from photooxidation of diiodomethane (CH_2I_2)". *J. Geophys. Res.* **2003**, *108* (D23), 4733; doi 10.1029/2003JD004249.
(28) Allan, J. D.; Coe, H.; Bower, K. N.; Alfarra, M. R.; Delia, A. E.; Jimenez, J. L.; Middlebrook, A. M.; Drewnick, F.; Onasch, T. B.; Canagaratna, M. R.; Jayne, J. T.; Worsnop, D. R. Technical note: Extraction of chemically resolved mass spectra from Aerodyne aerosol mass spectrometer data. *J. Aerosol Sci.* **2004**, *35*, 909−922.
(29) Alfarra, M. R.; Coe, H.; Allan, J. D.; Bower, K. N.; Boudries, H.; Canagaratna, M. R.; Jimenez, J. L.; Jayne, J. T.; Garforth, A.; Li, S.-M.; Worsnop, D. R. Characterization of urban and regional organics aerosols in the Lower Fraser Valley using two Aerodyne aerosol mass spectrometers. *Atm. Environ.* **2004**, *38*, 5745−5758.
(30) Hogrefe, O.; Drewnick, F.; Lala, G. G.; Schwab, J. J.; Demerjian, K. L. Development, Operation and Applications of an Aerosol Generation, Calibration and Research Facility. *Aerosol Sci. Technol.* **2004**, *38*, 196−214.
(31) Schneider et al. Biomass burning aerosol and other combustion derived particles: Composition, shape and density inferred from mass spectrometric measurements. Manuscript in preparation, 2005.
(32) Wehner, B.; Philippin, S.; Wiedensohler, A. Design and calibration of a thermodenuder with an improved heating unit to measure the size-dependent volatile fraction of aerosol particles. *J. Aerosol Sci.* **2002**, *33*, 1087−1093.
(33) Slowik, J. G.; Stainken, K.; Davidovits, P.; Williams, L. R.; Jayne, J. T.; Kolb, C. E.; Worsnop, D. R.; Rudich, Y.; DeCarlo, P.; Jimenez, J. L. Particle morphology and density characterization by combined mobility and aerodynamic diameter measurements. Part 2: Application to combustion-generated soot aerosols as a function of fuel equivalence ratio. *Aerosol Sci. Technol.* **2004**, *38*, 1206−1222.

Received for review April 16, 2004. Revised manuscript received March 8, 2005. Accepted May 25, 2005.

ES049427M